



Selective targeting of IRF4 by synthetic microRNA-125b-5p mimics induces anti-multiple myeloma activity in vitro and in vivo **OPEN**

E Morelli, E Leone, M E G Cantafio, M T Di Martino, N Amodio, L Biamonte, A Gullà, U Foresta, M Rita Pitari, C Botta, M Rossi, A Neri, N C Munshi, K C Anderson, P Tagliaferri, P Tassone

Cite this article as: E Morelli, E Leone, M E G Cantafio, M T Di Martino, N Amodio, L Biamonte, A Gullà, U Foresta, M Rita Pitari, C Botta, M Rossi, A Neri, N C Munshi, K C Anderson, P Tagliaferri, P Tassone, Selective targeting of IRF4 by synthetic microRNA-125b-5p mimics induces anti-multiple myeloma activity in vitro and in vivo, *Leukemia* accepted article preview 19 May 2015; doi: [10.1038/leu.2015.124](https://doi.org/10.1038/leu.2015.124).

This is a PDF file of an unedited peer-reviewed manuscript that has been accepted for publication. NPG are providing this early version of the manuscript as a service to our customers. The manuscript will undergo copyediting, typesetting and a proof review before it is published in its final form. Please note that during the production process errors may be discovered which could affect the content, and all legal disclaimers apply.



This work is licensed under a Creative Commons Attribution-NonCommercial-NoDerivs 4.0 International License. The images or other third party material in this article are included in the article's Creative Commons license, unless indicated otherwise in the credit line; if the material is not included under the Creative Commons license, users will need to obtain permission from the license holder to reproduce the material. To view a copy of this license, visit <http://creativecommons.org/licenses/by-nc-nd/4.0/>

Received 19 February 2015; revised 27 April 2015; accepted 5 May 2015;
Accepted article preview online 19 May 2015

Selective targeting of IRF4 by synthetic microRNA-125b-5p mimics induces anti-multiple myeloma activity *in vitro* and *in vivo***Running title:** miR-125b-5p exerts anti-myeloma activity

Eugenio Morelli, MD¹, Emanuela Leone, PhD¹, Maria Eugenia Gallo Cantafio, PhD¹, Maria Teresa Di Martino, PhD¹, Nicola Amodio, PhD¹, Lavinia Biamonte, PhD¹, Annamaria Gullà, MD¹, Umberto Foresta, PhD¹, Maria Rita Pitari, PhD¹, Cirino Botta, MD¹, Marco Rossi, MD¹, Antonino Neri, MD², Nikhil C. Munshi, MD^{3,4}, Kenneth C. Anderson, MD³, Pierosandro Tagliaferri, MD¹, and Pierfrancesco Tassone, MD^{1,5}

¹Department of Experimental and Clinical Medicine, Magna Graecia University, Salvatore Venuta University Campus, Catanzaro, Italy; ²Department of Medical Sciences, University of Milan, Hematology 1, IRCCS Policlinico Foundation, Milan, Italy; ³Jerome Lipper Multiple Myeloma Center, Department of Medical Oncology, Dana-Farber Cancer Institute, Boston, MA, USA; ⁴VA Boston Healthcare System, West Roxbury, Boston, MA, USA; ⁵Sbarro Institute for Cancer Research and Molecular Medicine, Center for Biotechnology, College of Science and Technology, Temple University, Philadelphia, PA, US.

Corresponding authors: Pierfrancesco Tassone, MD, Magna Graecia University, Viale Europa, 88100 Catanzaro, Italy; E-mail: tassone@unicz.it, Phone: +39-0961-3697029, Fax: +39-0961-3697341.

Conflict of Interest Disclosures: The authors declare no competing financial interests.

Fundings: This work has been supported by funds of Italian Association for Cancer Research (AIRC), PI: PT. "Special Program Molecular Clinical Oncology - 5 per mille" n. 9980, 2010/15. This work has also been supported by a grant from NIH PO1-155258, RO1-124929, P50-100007, PO1-78378 and VA merit grant IO1-24467.

Abstract:

Interferon regulatory factor 4 (IRF4) is an attractive therapeutic target in multiple myeloma (MM). We here report that expression of IRF4 mRNA inversely correlates with microRNA (miR)-125b in MM patients. Moreover, we provide evidence that miR-125b is downregulated in TC2/3 molecular MM subgroups and in established cell lines. Importantly, constitutive expression of miR-125b-5p by lentiviral vectors or transfection with synthetic mimics impaired growth and survival of MM cells and overcame the protective role of bone marrow stromal cells (BMSCs) *in vitro*. Apoptotic and autophagy-associated cell death were triggered in MM cells upon miR-125b-5p ectopic expression. Importantly, we found that the anti-MM activity of miR-125b-5p was mediated *via* direct downregulation of IRF4 and its downstream effector BLIMP-1. Moreover, inhibition of IRF4 translated into downregulation of c-Myc, caspase-10 and cFlip, relevant IRF4-downstream effectors. Finally, *in vivo* intra-tumor or systemic delivery of formulated miR-125b-5p mimics against human MM xenografts in SCID/NOD mice induced significant anti-tumor activity and prolonged survival. Taken together, our findings provide evidence that miR-125b, differently from other hematologic malignancies, has tumor suppressor activity in MM. Furthermore, our data provide proof-of-concept that synthetic miR-125b-5p mimics are promising anti-MM agents to be validated in early clinical trials.

Introduction

Multiple myeloma (MM) is a genetically complex malignancy from the outset, with progressive acquisition of genetic lesions mediating drug-resistance and high disease burden¹. Despite recent progress in the understanding MM pathobiology and the availability of innovative drugs which have improved clinical outcome, the disease eventually progresses to a drug-resistant lethal stage (plasma cell leukemia, PCL)²⁻⁴ and novel therapeutic strategies are therefore eagerly awaited. Indeed, one of the major challenges in treating MM is its genomic and phenotypic heterogeneity⁵. Hence, an optimal therapy would target an essential regulatory pathway shared by all disease subsets⁶.

Interferon regulatory factor 4 (IRF4) is a lymphocyte-specific transcription factor⁷. Interference with IRF4 expression is lethal for MM cells, irrespective of their genetics, making IRF4 an “Achilles’ heel” that may be exploited therapeutically⁸. Specifically, IRF4 is oncogenic and overexpressed when translocated to actively transcribed genomic regions in some MM patients, but it also plays a survival effect in MM cells in the absence of translocations or overexpression^{7, 8}. A relevant IRF4 target gene is *c-Myc*^{7, 8}, which has a prominent role in the pathogenesis of MM⁹. Another downstream IRF4 effector is *B lymphocyte induced maturation protein-1* (BLIMP-1)⁹: indeed, knockdown of BLIMP-1 causes apoptosis in MM cells. These findings suggest that IRF4 may regulate MM cell survival through modulation of BLIMP-1⁹. Moreover, it has been recently demonstrated that caspase-10 (*casp-10*) and *cFlip* genes are transactivated by IRF4: importantly, the evidence that all MM cell lines require *casp-10* and *cFLIP* for survival leads to the hypothesis that loss of the proteolytic activity of the *casp-10* / *cFlip* heterodimer mediates MM cell death induced by IRF4 knockdown¹⁰. All these data indicate IRF4 as an attractive therapeutic target in MM. However, efficient *in vivo* strategies aimed at blocking IRF4 pathway are still lacking.

MicroRNAs (miRNAs) are small non-coding RNAs of 19-25 nucleotides, which regulate gene expression by degrading or inhibiting translation of target mRNAs, primarily *via* base pairing to partially or fully complementary sites in the 3'UTR¹¹. Targeting deregulated miRNAs in cancer cells is emerging as a novel promising therapeutic approach¹²⁻¹⁴, including in MM¹⁵⁻³⁴. In this scenario, replacement of tumor-suppressor miRNAs by synthetic oligonucleotides (miRNA mimics) offers a new therapeutic opportunity to restore a loss of function in cancer, that has been an unmet need for drug developers³⁵.

Here, we show that IRF4 expression is regulated by microRNA-125b-5p (miR-125b-5p) in patient-derived MM cells and MM cell lines. In most of these cells, enforced expression of miR-125b-5p affects growth and survival, acting *via* IRF4 downregulation and impairment of its downstream signaling. Overall, our findings demonstrate that miR-125b is a tumor suppressor in MM, and provide the rationale for development of miR-125b-5p mimics as novel therapeutics.

Accepted manuscript

MM patient cells and cell lines

Following Magna Graecia University IRB study approval, primary MM cells were isolated from BM aspirates, as described¹⁹, from 24 newly diagnosed MM patients who had provided the informed consent. For transfection purposes and proliferation/survival assays, PBMCs from healthy donors have been used as controls. MM cell lines were cultured as described¹⁹. HS-5 human stromal cell line (purchased from ATCC, CRL-11882™) was cultured in DMEM supplemented with 10% fetal bovine serum and 1% penicillin/streptomycin .

Virus Generation and Infection of cells.

Cells stably expressing GFP transgene were obtained as described²¹. To generate cells stably expressing luciferase transgene, NCI-H929 cells were transduced with pLenti-III-PGK-Luc (ABM Inc.) vector. MM cells stably expressing miR-125b-1 and miR-125b-2 genes were transduced with Lenti-miR-125b-1 and Lenti-miR-125b-2 microRNA precursor constructs (system Biosciences, CA, US); lentiviral particles were produced and transduced as previously described¹⁹.

RNA extraction and quantitative real-time-PCR.

RNA samples of healthy donors bone marrow-derived plasma cells (hdPC) were purchased (AllCells). Total RNA extraction from MM cells and qRT-PCR were performed as previously described¹⁹.

In vitro transfection of MM cells

Synthetic miRNA mimics were purchased from Ambion (Applied Biosystems), while synthetic miRNA inhibitors were purchased from Exiqon (Vedbaek, Denmark). *Silencer*[®]Select siRNAs were purchased from Ambion (Applied Biosystems). All the oligos were used at 100 nmol/L final concentration. A total of $2,5 \times 10^5$ cells were transfected using Neon Transfection System (Invitrogen) (2 pulse at 1.050 V, 30 milliseconds) and the transfection efficiency, evaluated by flow-cytometric analysis relative to a FAM dye-

labeled miRNA inhibitor negative control, reached 85% to 90%. The same conditions were applied for transfection of MM cells with 5 µg of expression vectors carrying the ORFs of BLIMP-1 (EX-Z5827-M11), IRF4 (EX-M0891-M11) or empty vector (EX-EGFP-M11) (GeneCopeia, Rockville, MD, USA).

Survival assay

Cell viability was evaluated by Cell Counting Kit-8 (CCK-8) assay (Dojindo Molecular Technologies) and 7-Aminoactinomycin (7-AAD) flow cytometry assay (BD biosciences), according to manufacturer's instructions.

Detection of apoptosis

Apoptosis was investigated by three different assays: Annexin V/7-AAD flow cytometry assay, TUNEL assay and western blot analysis of caspases expression and cleavage.

Western blot analysis

Whole cell protein extracts were prepared from MM cell lines and from PBMCs in NP40 CellLysis Buffer (Novex®) containing a cocktail of protease inhibitors (Sigma, Steinheim, Germany). Cell lysates were loaded and PAGE separated. Proteins were transferred by Trans-Blot® Turbo™ Transfer Starter System for 7 min. After protein transfer, the membranes were blotted with the primary antibodies (see supplemental methods for detailed informations).

Animals and *in vivo* model of human MM

Male CB-17 severe combined immunodeficient (SCID) mice (6- to 8-weeks old; Harlan Laboratories, Inc., Indianapolis) were housed and monitored in our Animal Research Facility. Experimental procedures and protocols had been approved by the Magna Graecia University IRB and conducted according to protocols approved by the National Directorate of Veterinary Services (Italy). Mice were sc inoculated with 5×10^6 NCI-H929 cells and treatment started when palpable tumors became detectable. Sample size was chosen accordingly to our experience¹⁶⁻²⁰. Tumor sizes were measured as described¹⁹, and the investigator was blinded to group allocation. Tumor size of luciferase gene-marked NCI-

H929 xenografts were also measured by IVIS Lumina II. Oligos were NLE-formulated within MaxSuppressor In Vivo LANCER II (Bilo Scientific) to achieve an efficient delivery, as reported^{16, 27}.

Statistical Analysis

Each experiment was performed at least 3 times and values are reported as means \pm SD. Comparisons between groups were made with student's t-test, while statistical significance of differences among multiple groups was determined by GraphPad software (www.graphpad.com). Graphs were obtained using Graphpad Prism version 6.0. p-value of less than 0.05 was accepted as statistically significant.

Accepted manuscript

1. Inverse correlation between IRF4 mRNA and miR-125b in MM patients

To identify IRF4 targeting miRNAs, we interrogated *microRNA Data Integration Portal* (mirDIP), applying the *high precision* quality filter³⁶. As shown in Table 1, this analysis disclosed 12 mature miRNAs including miR-125a-5p, miR-125b-5p, miR-128, miR-27a-3p, miR-27b-3p, miR-30a-5p, miR-30b-5p, miR-30c-2, miR-30d-5p, miR-30e-5p, miR-4319 and miR-513a-5p. We next attempted to correlate the expression of these miRNAs and IRF4 mRNA in our dataset (55 MM and 21 PCL patients)(GSE39925). This integrated approach revealed a significant inverse correlation between IRF4 mRNA and five precursor-miRNAs (pre-miR-125b-1, pre-miR-125b-2, pre-miR-30b, pre-miR-30c-2 and pre-miR-30d) among all MM and PCL patients examined (Fig. 1A-B and Fig. S1A). Importantly, when a second dataset (GSE47552) was interrogated, the inverse correlation with IRF4 mRNA was confirmed only for pre-miR-125b-1 (Fig. S1B), strengthening a possible role of miR-125b-5p as IRF4 negative regulator in MM patients. By qRT-PCR, we then evaluated the expression of miR-125b-5p in 24 CD138⁺ primary patient MM (ppMM) cells, 10 MM cell lines and 3 samples of CD138⁺ BM-derived plasma cells from healthy donors (HD-PCs). A significant downregulation of miR-125b-5p was found in MM cell lines (Fig. 1C, with single values plotted in Fig. S2), while the downregulatory trend observed in ppMM cells reached statistical significance within the TC2 and TC3 subgroups only (Fig. 1C-D).

2. Enforced expression of miR-125b impairs growth and survival of MM cells

To evaluate the effects induced by miR-125b, we transduced 3 MM cell lines (NCI-H929, SK-MM-1, RPMI-8226) with lentiviral vectors carrying either miR-125b-1 or miR-125b-2 (Lenti-miR-125b-1 or Lenti-miR-125b-2) genes. The effects on cell proliferation were assessed by CCK-8 assay at 2, 3 and 4 days after selection by puromycin. As shown in Fig. 2A-B, constitutive expression of either Lenti-miR-125b-1 or Lenti-miR-125b-2 resulted in a strong inhibition of cell growth. Next, we transfected MM cell lines with either synthetic miR-125b-5p mimics or inhibitors. We found that ectopic expression of miR-125b-5p inhibitors did not affect the proliferation of MM cells (Fig. 2C-D); conversely, transfection of

miR-125b-5p mimics strongly impaired growth and survival of most MM cell lines (9 out of 10) (Fig. 2E-F). Importantly, miR-125b-5p mimics reduced the viability of ppMM cells from 3 individuals (Fig. 2G), but not of PBMCs from 6 healthy donors (Fig. 2H). Taken together, these results indicate that enforced expression of miR-125b-5p inhibits growth and survival of MM cells, consistent with a tumor-suppressor function of miR-125b in MM cells. Notably, baseline expression of miR-125b-5p did not correlate with the sensitivity/response to synthetic mimics or inhibitors, suggesting that miR-125b-5p expression is not predictive of *in vitro* anti-MM activity. Furthermore, miR-125b-5p mimics were lethal to MM cells irrespective of their genetics.

3. miR-125b-5p mimics inhibit proliferation of MM cells *via* targeting IRF4

To investigate whether IRF4 expression could be affected by ectopic miR-125b-5p, both qRT-PCR and western blot analysis were performed in 3 MM cell lines transfected with miR-125b-5p mimics or scrambled controls (miR-NC). Specifically, the IRF4 translocated SK-MM-1, along with NCI-H929 and RPMI-8226 cells (not IRF4 translocated), were selected for this analysis. As shown in Fig. 3A-B, transfection of miR-125b-5p downregulated IRF4 at both mRNA and protein levels in all MM cell lines. Notably, the only MM cell line resistant to miR-125b-5p overexpression lacked detectable IRF4 (i.e. RPMI-8226/Dox40 cells, which were generated from the parental RPMI-8226 by continuous exposure to increasing amounts of doxorubicin to culture medium, is characterized by loss of miR-125b-5p relevant targets) (Fig. S3A). Consistently, we found that viability of RPMI-8226/Dox40 cells was not affected by IRF4 siRNA silencing (Fig. S3B); in contrast siRNA-transfection of both NCI-H929 and SK-MM-1 cells confirmed its role in supporting their survival (Fig. S3B). We next investigated whether ectopic expression of a cDNA containing only the coding region of IRF4 and lacking the miR-125b-5p-targeted 3'UTR regions could protect MM cells from miR-125b-5p anti-proliferative effects. As shown in Fig. 3C, transfection of IRF4 construct increased IRF4 protein expression which was not affected by miR-125b-5p mimics. Importantly, IRF4 overexpression rescued SK-MM-1 cells from the growth-inhibitory activity of either IRF4 siRNAs (Fig. S3C) or miR-125b-5p mimics (Fig. 3D), indicating that miR-125b exerts its anti-MM activity *via* targeting IRF4.

4. Enforced expression of miR-125b-5p impairs IRF4 signaling in MM cell lines

We next investigated the effects of miR-125b-5p on the molecular network underlying IRF4 activity in MM. Interestingly, the IRF4 downstream effector BLIMP-1 has been proven to be a direct target of miR-125b-5p³⁷. As shown in Fig. 4A and Fig. S4A, transfection of miR-125b-5p mimics downregulated BLIMP-1 protein in SK-MM-1 and NCI-H929 cells. Thus, we investigated whether ectopic expression of a cDNA containing only the coding region of BLIMP-1 and lacking the miR-125b-5p-targeted 3'UTR regions could protect MM cells from miR-125b-5p effects. Importantly, co-transfection with BLIMP-1 construct weakened the anti-proliferative effect of miR-125b-5p mimics as well of BLIMP-1 siRNAs (Fig. 4C and Fig. S4B), indicating that also BLIMP-1 mediates the anti-MM activity of miR-125b-5p. Of note, miR-125b-5p-induced downregulation of BLIMP-1 was not abrogated in SK-MM-1 cells co-transfected with the coding region of IRF4 (Fig. 4B), consistent with the notion that BLIMP-1 is a direct target of miR-125b-5p which circumvents IRF4 activity on BLIMP1. Other IRF4 downstream effectors, with a prominent role in MM pathogenesis, are c-Myc, caspase-10 (casp-10) and cFLIP^{8, 10}. By western blot analysis, we found reduced expression of these proteins in SK-MM-1 (Fig. 4D) and NCI-H929 (Fig. S4E) cells at 24-48h after transfection with miR-125b-5p. Expression of both casp-10 and cFlip was also reduced at mRNA levels (Fig. S4F) by miR-125b-5p mimics. *In silico* search for target prediction identified both casp-10 and cFlip as *bona fide* direct targets for miR-125b-5p. To validate this interaction in MM cells, SK-MM-1 cells were co-transfected with miR-125b-5p mimics or scrambled oligonucleotides, together with an expression vector carrying the 3'UTR of casp-10 or cFlip mRNA cloned downstream of luciferase reporter gene. Of note, we did not find significant changes in 3' UTR luciferase activity after miR-125b-5p overexpression, ruling out direct targeting of casp-10 and cFlip mRNAs by miR-125b-5p (Fig. S4G). Moreover, miR-125b-5p-induced downregulation of c-Myc, casp-10 and cFlip was abrogated in SK-MM-1 cells co-transfected with the coding region of IRF4 (Fig. 4E), indicating that miR-125b-5p-induced downregulation of casp-10, c-Myc and cFlip occurs *via* IRF4 inhibition. Taken together, our findings demonstrate that miR-125b-5p mimics impair IRF4 signaling in MM cells (Fig. 4F). We also found that direct targeting of IRF4 or BLIMP-1 and indirect modulation of c-Myc, casp-10 and cFlip mediates anti-MM activity of this miRNA.

5. miR-125b-5p mimics trigger both apoptotic and autophagy-associated cell death

Inhibition of IRF4, as well of BLIMP-1 or c-Myc, has been mainly related to induction of apoptosis^{9, 38}, while targeting casp-10 or its interaction with cFlip triggers autophagic cell death of MM cells¹⁰. On this basis, we next determined whether apoptotic or autophagy-associated cell death occurred in MM cells with enforced expression of miR-125b-5p. Using Annexin V/7-AAD flow cytometry assay, we found that miR-125b-5p mimics triggered exposure of phosphatidylserine (PS) and phosphatidylethanolamine (PE) on the cell surface of SK-MM-1 (Fig. 5A), NCI-H929 and U266 cells (Fig. S5A), followed by cell membrane disruption. Moreover, by TUNEL assay and western blotting, we found that miR-125b-5p induced DNA-fragmentation (Fig. S5B) and cleavage/activation of both initiator caspase-8 and effector caspase-3 (Fig. 5B and Fig. S5C) in MM cells. Of note, apoptosis was not detected when miR-125b-5p-transfected cells were treated with the pan-caspase inhibitor Z-VAD-fmk (Fig. 5C). Overall, these results indicate that miR-125b-5p is pro-apoptotic in MM cells. Moreover, by flow cytometry analysis of Cyto-ID stained cells, we observed an increase of autophagic vacuoles in SK-MM-1, XG-1 and INA-6 cells, at 48h after transfection with miR-125b-5p (Fig. 5D). Importantly, the increase of autophagic vacuoles occurred to a similar extent in cells transfected with miR-125b-5p compared with cells starved for 48 hours. Moreover, western blot analysis showed decreased p62/SQSTM1 and increased Beclin-1 and proteolytic active LCIIIB (Fig. 5E), further suggesting that miR-125b-5p-induced cell death can be associated with autophagy induction in MM cells. Indeed, exposure of miR-125b-5p-transfected cells to autophagy inhibitor cloroquine resulted in increased cell death (Fig. 5F), thus suggesting a protective role of autophagy in our experimental settings.

6. miR-125b-5p mimics antagonize the BMSCs protective role on MM cells

Bone marrow (BM) *milieu* strongly support survival and proliferation of MM cells³. In this regard, we found that exogenous IL-6 or IGF-1 or HGF significantly reduced miR-125b-5p expression in all MM cell lines except U266 cells (Fig. 6A), which express L-Myc instead of c-Myc. Since c-Myc suppresses miR-125b transcription^{39, 40} and is upregulated by IL-6, IGF-1 and HGF⁴⁰⁻⁴², we investigated whether these factors downregulate miR-125b in MM cells through c-Myc induction. Specifically, we treated c-Myc-expressing SK-MM-1 and c-Myc-defective U266 cells with the 10058-F4 small molecule inhibitor of Myc-Max

heterodimerization³⁸ and with the JQ1 BET-bromodomain inhibitor, which is reported to inhibit c-Myc transcription⁴³. Importantly, both compounds triggered a significant miR-125b-5p upregulation in SK-MM-1 cells, but not in U226 cells (Fig. 6B), indicating that c-Myc-independent downregulation of miR-125b occurs in this cell line. Moreover, IL-6 or IGF-1 or HGF didn't affect miR-125b-5p expression in SK-MM-1 cells in the presence of c-Myc inhibitors, indicating a c-Myc-mediated downregulation of miR-125b by exogenous addition of microenvironmental growth factors (Fig. 6C). Finally, we demonstrated that the anti-MM activity of miR-125b-5p mimics was not antagonized by exogenous growth promoting/pro-survival stimuli including IL-6, IGF-1, and HGF, nor by adherence of MM cell lines to HS-5 human stromal cells (Fig. 6D-E). This could be partly due to downregulation of IL-6R/CD126 on the surface of MM cells. Indeed, by flow cytometry analysis, we did observe decreased expression of cell surface IL-6R/CD126, also a further validated target of miR-125b-5p⁴⁴ (Fig. 6F), which translated in reduced levels of phosphorylated/active STAT3 (pSTAT3-Y705) in IL-6 dependent INA-6 cells (Fig. 6G).

7. *In vivo* delivery of NLE-formulated synthetic miR-125b-5p mimics exerts anti-MM activity

In vivo anti-MM activity of miR-125b-5p was next evaluated in NOD-SCID mice bearing subcutaneous NCI-H929 xenografts. In our first model, luciferase gene-marked NCI-H929 xenografts were intra-tumorally treated every other day with 1 mg/kg of oligos for a total of 6 injections. As shown in Fig. 7A-C, treatment resulted in a significant tumor-growth inhibition and prolonged survival. In a second model, treatments were administered by intra-peritoneal injections of formulated oligos (twice/weekly, 1 mg/kg). In this model, we also observed anti-tumor activity of miR-125b-5p, evidenced by growth inhibition and prolonged survival (Fig. 7D-E). Importantly, we found increased miR-125b-5p in tumors retrieved from animals 48h after treatment, confirming efficient tumor cells uptake of formulated oligos (Fig. 7F). Consistent with our *in vitro* data, IRF4 signaling was correlated with miR-125b-5p activity *in vivo*: downregulation of IRF4 and BLIMP-1 (Fig. 7G), along with decreased expression of c-Myc, casp-10 and cFlip proteins (Fig. 7H), was detected in tumors retrieved from miR-125b-5p treated animals. Overall, these data indicate that *in vivo* anti-MM activity of miR-125b-5p mimics is associated with abrogation of IRF4 signaling within MM xenografts.

Discussion

In this study, we investigated the anti-MM activity of the IRF4-targeting miR-125b-5p. IRF4 is in fact an “Achilles’ heel” for MM cells and, therefore, represents an attractive therapeutic target in this malignancy⁷. miRNAs are natural antisense interactors of mRNAs, and the availability of suitable *in vivo* delivery systems has recently allowed the development of synthetic miRNA mimics in early clinical trials. By querying *microRNA Data Integration Portal* (mirDIP)³⁶ and applying the *high precision* quality filter, we found 12 mature miRNAs predicted to target the 3’UTR of IRF4 mRNA, including miR-125b-5p. Importantly, integrated analysis of miRNAs and mRNAs expression profiles showed that miR-125b, but not the other predicted miRNAs, inversely correlated with IRF4 mRNA in 2 different MM datasets, strengthening the relevance of miR-125b as IRF4 negative regulator in MM patients. Furthermore, miR-125b-5p was found significantly downregulated in patients belonging to TC2 and TC3 molecular subgroups, as well as in MM cell lines. Altogether, these findings prompted us to investigate the role of this miRNA in MM.

miR-125b is one of the most evolutionary conserved miRNAs⁴⁵. In humans there are 2 paralogs (hsa-miR-125b-1 on chromosome 11 and hsa-miR-125b-2 on chromosome 21), coding for the same mature sequences (miR-125b-5p and miR-125b-3p)⁴⁵. miR-125b plays a crucial role in a variety of cellular processes and diseases⁴⁶. It is commonly dysregulated in cancer⁴⁶, but its function diverges in different malignancies, with dependence on the molecular contexts. However, its role in MM is still largely undisclosed⁴⁶⁻⁴⁸.

We here provide the evidence that miR-125b acts as tumor suppressor in MM *via* targeting IRF4 and BLIMP-1 mRNAs, and importantly, we show that NLE-formulated synthetic miR-125b-5p mimics induce anti-tumor activity *in vivo*. Specifically, we demonstrate that both lentivirus-based constitutive expression of miR-125b-1/-2 genes and transient enforced expression of synthetic miR-125b-5p mimics inhibit the growth and survival of MM cell lines. Moreover, viability of ppMM cells, but not of PBMCs from healthy donors, was affected by transfection with miR-125b-5p mimics, suggesting a favorable therapeutic activity. In our study, baseline expression of miR-125b-5p does not correlate with *in vitro* sensitivity of MM cells to synthetic mimics; consistent with our findings, increasing evidence demonstrate that cancer cells with normal miRNA expression are indeed susceptible to miRNA treatment³⁵. Importantly, the anti-MM activity of miR-125b-5p

mimics was not affected by either exogenous growth promoting/pro-survival stimuli including IL-6, IGF-1, or HGF, or by adherence of MM cell lines to BMSCs. This is a crucial point taking into account that the close and dynamic interplay between MM cells and BMSCs leads to activation of signal transduction pathways which promote cell cycle progression and protection from apoptosis³. Furthermore, a c-Myc-mediated downregulation of miR-125b by exposure of MM cells to different growth factors was observed.

To date, a variety of oncogenic pathways have been identified as directly regulated by miR-125b^{46, 47}. Here, we demonstrate a functional link between this miRNA and the oncogenic IRF4 signaling in MM. IRF4 is a validated target of miR-125b-5p^{37, 49} and the relevance of this interaction is well established in both myeloid- and B-cells leukemias, wherein IRF4 acts as tumor-suppressor and miR-125b as tumor-promoter⁵⁰. We found that IRF4 expression was downregulated upon transfection of MM cells with miR-125b-5p mimics. Among the MM cell lines studied, only miR-125b-5p-resistant RPMI-8226/Dox40 cells did not express detectable levels of IRF4. Importantly, overexpression of IRF4 was able to rescue SK-MM-1 cells from the growth-inhibitory activity of miR-125b-5p. Altogether, these data indicate that IRF4 mediates the anti-MM activity of miR-125b-5p mimics *in vitro*, underlying a novel and divergent role of miR-125b-5p/IRF4 axis in MM as compared to other hematological malignancies.

miRNAs function as master regulators of the genome by modulating the expression of tens to hundreds genes, often belonging to the same pathway³⁵. This mechanism of action provides advantage to the therapeutic use of miRNAs, since it is consistent with the current vision of cancer as a pathway disease³⁵. Interestingly, the IRF4 downstream effector BLIMP-1 is also regulated by miR-125b-5p³⁷, and we demonstrated that, similar to IRF4 but at lesser extent, it also mediate the growth-inhibitory activity of miR-125b-5p. Moreover, we analyzed perturbations occurring in other relevant effectors of IRF4 signaling, including c-Myc, casp-10 and cFlip. c-Myc plays a prominent role in the pathogenesis of MM, wherein it represents an attractive therapeutic target^{7, 38, 43}. Importantly, ectopic expression of miR-125b-5p significantly decreased c-Myc protein in MM cells which was rescued by co-transfection with the coding region of IRF4, indicating that IRF4 mediates miR-125b-5p-triggered downregulation of c-Myc. Recently, it has been demonstrated that MM cells further require the IRF4 downstream effectors casp-10 and cFlip for their survival: indeed, the heterodimeric protease composed of casp-10 and cFLIP proteins plays a balancing role among the pro-survival and pro-death effects of autophagy¹⁰.

Consistent with these notions, we found that both casp-10 and cFlip undergo significant downregulation upon miR-125b-5p ectopic expression in MM cells, along with increased autophagic flux. Nonetheless, the role of autophagy as a response to miR-125b-5p overexpression points to further investigation, taking into account that our present data indeed suggest a protective effect at least in SK-MM-1 cells. Even though *in silico* search for target prediction indicated both casp-10 and cFlip as *bona fide* direct targets for miR-125b-5p, we failed to validate this interaction. However, miR-125b-5p-induced downregulation of casp-10 and cFlip was abrogated by ectopic IRF4 expression, indicating that miR-125b-5p-mediated downregulation of these 2 survival factors depends on IRF4 targeting.

Finally, we demonstrated the *in vivo* anti-tumor activity of NLE-formulated miR-125b-5p mimics against human MM xenografts in SCID/NOD mice. To our knowledge, this is the first evidence of a successful *in vivo* treatment with miR-125b-5p mimics in a murine xenograft model of human MM, which indeed has important potential towards clinical applications. We showed that both intra-tumor and intra-peritoneal injection of NLE-formulated miR-125b-5p mimics resulted in significant tumor-growth inhibition and prolonged survival. Moreover, in tumors retrieved from animals treated with miR-125b-5p mimics, a down-regulation of its direct targets IRF4 and BLIMP-1, along with a reduction in expression of c-Myc, casp-10 and cFlip proteins, was observed. These findings suggest that the *in vivo* anti-MM activity of miR-125b-5p mimics is related to the impairment of IRF4-signaling within MM xenografts. Further *in vivo* evaluation in preclinical models recapitulating the huBMM, such as the SCID-synth-hu⁵¹, will strengthen the translational value of miR-125b-5p mimics.

We think that our study provides important proof-of-concept findings for the basic strategy of miRNA therapeutics. In fact, we found that the miR-125b-5p/IRF4 axis has a highly disease specific functional role in MM which runs in opposite directions as compared with other hematological malignancies. These findings support the peculiarity of MM BM microenvironment disease scenario which opens highly specific therapeutic avenues. An additional important point is that miR-125b-5p strongly inhibits both IRF4 and BLIMP1, offering a pathway directed therapeutic tool, which is still undruggable by alternative approaches. In conclusion, our investigation provides evidence that miR-125b-5p has tumor suppressor activity in MM and that enforced expression of synthetic miR-125b-5p mimics induces significant anti-MM activity *in vitro and in vivo* by IRF4 targeting. Taken

together, these results provide the rational framework for development of miR-125b-5p-based therapies in MM.

Acknowledgments: This work has been supported by funds of Italian Association for Cancer Research (AIRC), PI: PT. "Special Program Molecular Clinical Oncology - 5 per mille" n. 9980, 2010/15. This work has also been supported by a grant from NIH PO1-155258, RO1-124929, P50-100007, PO1-78378 and VA merit grant IO1-24467.

Authorship Contributions: EM, EL, MEGC, MTDM, NA, LB, AG, UF, MRP, CB and MR performed experiments and analyzed the data; AN provided biological samples; PT and PT conceived the study; EM, PT and PT wrote the manuscript; NCM and KCA provided critical evaluation of experimental data and manuscript.

Conflict of Interest Disclosures: The authors declare no competing financial interests.

'Supplementary information is available at Leukemia's website'

References

1. Anderson KC, Carrasco RD. Pathogenesis of myeloma. *Annual review of pathology* 2011; **6**: 249-274.
2. Rajkumar SV. Treatment of multiple myeloma. *Nature reviews Clinical oncology* 2011 Aug; **8**(8): 479-491.
3. Podar K, Chauhan D, Anderson KC. Bone marrow microenvironment and the identification of new targets for myeloma therapy. *Leukemia* 2009 Jan; **23**(1): 10-24.
4. Rossi M, Di Martino MT, Morelli E, Leotta M, Rizzo A, Grimaldi A, *et al.* Molecular targets for the treatment of multiple myeloma. *Current cancer drug targets* 2012 Sep; **12**(7): 757-767.
5. Morgan GJ, Walker BA, Davies FE. The genetic architecture of multiple myeloma. *Nature reviews Cancer* 2012 May; **12**(5): 335-348.
6. Kuehl WM, Bergsagel PL. Molecular pathogenesis of multiple myeloma and its premalignant precursor. *The Journal of clinical investigation* 2012 Oct; **122**(10): 3456-3463.
7. Shaffer AL, Emre NC, Romesser PB, Staudt LM. IRF4: Immunity. Malignancy! Therapy? *Clinical cancer research : an official journal of the American Association for Cancer Research* 2009 May 1; **15**(9): 2954-2961.
8. Shaffer AL, Emre NC, Lamy L, Ngo VN, Wright G, Xiao W, *et al.* IRF4 addiction in multiple myeloma. *Nature* 2008 Jul 10; **454**(7201): 226-231.
9. Lin FR, Kuo HK, Ying HY, Yang FH, Lin KI. Induction of apoptosis in plasma cells by B lymphocyte-induced maturation protein-1 knockdown. *Cancer research* 2007 Dec 15; **67**(24): 11914-11923.
10. Lamy L, Ngo VN, Emre NC, Shaffer AL, 3rd, Yang Y, Tian E, *et al.* Control of autophagic cell death by caspase-10 in multiple myeloma. *Cancer cell* 2013 Apr 15; **23**(4): 435-449.
11. Bartel DP. MicroRNAs: genomics, biogenesis, mechanism, and function. *Cell* 2004 Jan 23; **116**(2): 281-297.
12. Garzon R, Marcucci G, Croce CM. Targeting microRNAs in cancer: rationale, strategies and challenges. *Nature reviews Drug discovery* 2010 Oct; **9**(10): 775-789.
13. Trang P, Weidhaas JB, Slack FJ. MicroRNAs as potential cancer therapeutics. *Oncogene* 2008 Dec; **27 Suppl 2**: S52-57.
14. Misso G, Di Martino MT, De Rosa G, Farooqi AA, Lombardi A, Campani V, *et al.* Mir-34: a new weapon against cancer? *Molecular therapy Nucleic acids* 2014; **3**: e194.

15. Amodio N, Di Martino MT, Neri A, Tagliaferri P, Tassone P. Non-coding RNA: a novel opportunity for the personalized treatment of multiple myeloma. *Expert opinion on biological therapy* 2013 Jun; **13** Suppl 1: S125-137.
16. Di Martino MT, Leone E, Amodio N, Foresta U, Lionetti M, Pitari MR, *et al.* Synthetic miR-34a mimics as a novel therapeutic agent for multiple myeloma: in vitro and in vivo evidence. *Clinical cancer research : an official journal of the American Association for Cancer Research* 2012 Nov 15; **18**(22): 6260-6270.
17. Di Martino MT, Gulla A, Gallo Cantafio ME, Altomare E, Amodio N, Leone E, *et al.* In vitro and in vivo activity of a novel locked nucleic acid (LNA)-inhibitor-miR-221 against multiple myeloma cells. *PloS one* 2014; **9**(2): e89659.
18. Di Martino MT, Gulla A, Cantafio ME, Lionetti M, Leone E, Amodio N, *et al.* In vitro and in vivo anti-tumor activity of miR-221/222 inhibitors in multiple myeloma. *Oncotarget* 2013 Feb; **4**(2): 242-255.
19. Leone E, Morelli E, Di Martino MT, Amodio N, Foresta U, Gulla A, *et al.* Targeting miR-21 inhibits in vitro and in vivo multiple myeloma cell growth. *Clinical cancer research : an official journal of the American Association for Cancer Research* 2013 Apr 15; **19**(8): 2096-2106.
20. Amodio N, Di Martino MT, Foresta U, Leone E, Lionetti M, Leotta M, *et al.* miR-29b sensitizes multiple myeloma cells to bortezomib-induced apoptosis through the activation of a feedback loop with the transcription factor Sp1. *Cell death & disease* 2012; **3**: e436.
21. Leotta M, Biamonte L, Raimondi L, Ronchetti D, Di Martino MT, Botta C, *et al.* A p53-dependent tumor suppressor network is induced by selective miR-125a-5p inhibition in multiple myeloma cells. *Journal of cellular physiology* 2014 Dec; **229**(12): 2106-2116.
22. Zhao JJ, Lin J, Zhu D, Wang X, Brooks D, Chen M, *et al.* miR-30-5p functions as a tumor suppressor and novel therapeutic tool by targeting the oncogenic Wnt/beta-catenin/BCL9 pathway. *Cancer research* 2014 Mar 15; **74**(6): 1801-1813.
23. Misiewicz-Krzeminska J, Sarasquete ME, Quwaider D, Krzeminski P, Ticona FV, Paino T, *et al.* Restoration of microRNA-214 expression reduces growth of myeloma cells through positive regulation of P53 and inhibition of DNA replication. *Haematologica* 2013 Apr; **98**(4): 640-648.
24. Pichiorri F, Suh SS, Ladetto M, Kuehl M, Palumbo T, Drandi D, *et al.* MicroRNAs regulate critical genes associated with multiple myeloma pathogenesis. *Proceedings of the National Academy of Sciences of the United States of America* 2008 Sep 2; **105**(35): 12885-12890.
25. Pichiorri F, Suh SS, Rocci A, De Luca L, Taccioli C, Santhanam R, *et al.* Downregulation of p53-inducible microRNAs 192, 194, and 215 impairs the p53/MDM2 autoregulatory loop in multiple myeloma development. *Cancer cell* 2010 Oct 19; **18**(4): 367-381.
26. Rossi M, Amodio N, Di Martino MT, Tagliaferri P, Tassone P, Cho WC. MicroRNA and multiple myeloma: from laboratory findings to translational therapeutic approaches. *Current pharmaceutical biotechnology* 2014; **15**(5): 459-467.

27. Raimondi L, Amodio N, Di Martino MT, Altomare E, Leotta M, Caracciolo D, *et al.* Targeting of multiple myeloma-related angiogenesis by miR-199a-5p mimics: in vitro and in vivo anti-tumor activity. *Oncotarget* 2014 May 30; **5**(10): 3039-3054.
28. Scognamiglio I, Di Martino MT, Campani V, Virgilio A, Galeone A, Gulla A, *et al.* Transferrin-conjugated SNALPs encapsulating 2'-O-methylated miR-34a for the treatment of multiple myeloma. *BioMed research international* 2014; **2014**: 217365.
29. Di Martino MT, Campani V, Misso G, Gallo Cantafio ME, Gulla A, Foresta U, *et al.* In vivo activity of miR-34a mimics delivered by stable nucleic acid lipid particles (SNALPs) against multiple myeloma. *PLoS one* 2014; **9**(2): e90005.
30. Amodio N, Bellizzi D, Leotta M, Raimondi L, Biamonte L, D'Aquila P, *et al.* miR-29b induces SOCS-1 expression by promoter demethylation and negatively regulates migration of multiple myeloma and endothelial cells. *Cell Cycle* 2013 Dec 1; **12**(23): 3650-3662.
31. Lionetti M, Musto P, Di Martino MT, Fabris S, Agnelli L, Todoerti K, *et al.* Biological and clinical relevance of miRNA expression signatures in primary plasma cell leukemia. *Clinical cancer research : an official journal of the American Association for Cancer Research* 2013 Jun 15; **19**(12): 3130-3142.
32. Rossi M, Pitari MR, Amodio N, Di Martino MT, Conforti F, Leone E, *et al.* miR-29b negatively regulates human osteoclastic cell differentiation and function: implications for the treatment of multiple myeloma-related bone disease. *Journal of cellular physiology* 2013 Jul; **228**(7): 1506-1515.
33. Amodio N, Leotta M, Bellizzi D, Di Martino MT, D'Aquila P, Lionetti M, *et al.* DNA-demethylating and anti-tumor activity of synthetic miR-29b mimics in multiple myeloma. *Oncotarget* 2012 Oct; **3**(10): 1246-1258.
34. Tagliaferri P, Rossi M, Di Martino MT, Amodio N, Leone E, Gulla A, *et al.* Promises and challenges of MicroRNA-based treatment of multiple myeloma. *Current cancer drug targets* 2012 Sep; **12**(7): 838-846.
35. Bader AG. miR-34 - a microRNA replacement therapy is headed to the clinic. *Frontiers in genetics* 2012; **3**: 120.
36. Shirdel EA, Xie W, Mak TW, Jurisica I. NAViGaTing the micronome--using multiple microRNA prediction databases to identify signalling pathway-associated microRNAs. *PLoS one* 2011; **6**(2): e17429.
37. Gururajan M, Haga CL, Das S, Leu CM, Hodson D, Josson S, *et al.* MicroRNA 125b inhibition of B cell differentiation in germinal centers. *International immunology* 2010 Jul; **22**(7): 583-592.
38. Holien T, Vatsveen TK, Hella H, Waage A, Sundan A. Addiction to c-MYC in multiple myeloma. *Blood* 2012 Sep 20; **120**(12): 2450-2453.

39. Chang TC, Yu D, Lee YS, Wentzel EA, Arking DE, West KM, *et al.* Widespread microRNA repression by Myc contributes to tumorigenesis. *Nature genetics* 2008 Jan; **40**(1): 43-50.
40. Popowski M, Ferguson HA, Sion AM, Koller E, Knudsen E, Van Den Berg CL. Stress and IGF-I differentially control cell fate through mammalian target of rapamycin (mTOR) and retinoblastoma protein (pRB). *The Journal of biological chemistry* 2008 Oct 17; **283**(42): 28265-28273.
41. Shi Y, Frost P, Hoang B, Benavides A, Gera J, Lichtenstein A. IL-6-induced enhancement of c-Myc translation in multiple myeloma cells: critical role of cytoplasmic localization of the rna-binding protein hnRNP A1. *The Journal of biological chemistry* 2011 Jan 7; **286**(1): 67-78.
42. Li X, Bian Y, Takizawa Y, Hashimoto T, Ikoma T, Tanaka J, *et al.* ERK-dependent downregulation of Skp2 reduces Myc activity with HGF, leading to inhibition of cell proliferation through a decrease in Id1 expression. *Molecular cancer research : MCR* 2013 Nov; **11**(11): 1437-1447.
43. Delmore JE, Issa GC, Lemieux ME, Rahl PB, Shi J, Jacobs HM, *et al.* BET bromodomain inhibition as a therapeutic strategy to target c-Myc. *Cell* 2011 Sep 16; **146**(6): 904-917.
44. Gong J, Zhang JP, Li B, Zeng C, You K, Chen MX, *et al.* MicroRNA-125b promotes apoptosis by regulating the expression of Mcl-1, Bcl-w and IL-6R. *Oncogene* 2013 Jun 20; **32**(25): 3071-3079.
45. Shaham L, Binder V, Gefen N, Borkhardt A, Izraeli S. MiR-125 in normal and malignant hematopoiesis. *Leukemia* 2012 Sep; **26**(9): 2011-2018.
46. Sun YM, Lin KY, Chen YQ. Diverse functions of miR-125 family in different cell contexts. *Journal of hematology & oncology* 2013; **6**: 6.
47. Kumar M, Lu Z, Takwi AA, Chen W, Callander NS, Ramos KS, *et al.* Negative regulation of the tumor suppressor p53 gene by microRNAs. *Oncogene* 2011 Feb 17; **30**(7): 843-853.
48. Murray MY, Rushworth SA, Zaitseva L, Bowles KM, Macewan DJ. Attenuation of dexamethasone-induced cell death in multiple myeloma is mediated by miR-125b expression. *Cell cycle* 2013 Jul 1; **12**(13): 2144-2153.
49. Chaudhuri AA, So AY, Sinha N, Gibson WS, Taganov KD, O'Connell RM, *et al.* MicroRNA-125b potentiates macrophage activation. *Journal of immunology* 2011 Nov 15; **187**(10): 5062-5068.
50. So AY, Sookram R, Chaudhuri AA, Minisandram A, Cheng D, Xie C, *et al.* Dual mechanisms by which miR-125b represses IRF4 to induce myeloid and B-cell leukemias. *Blood* 2014 Aug 28; **124**(9): 1502-1512.
51. Calimeri T, Battista E, Conforti F, Neri P, Di Martino MT, Rossi M, *et al.* A unique three-dimensional SCID-polymeric scaffold (SCID-synth-hu) model for in vivo expansion of human primary multiple myeloma cells. *Leukemia* 2011 Apr; **25**(4): 707-711.

Figure Legends

Figure 1. miR-125b inversely correlate with IRF4 mRNA in MM patients. Analysis of IRF4 mRNA and either (A) miR-125b-1 or (B) miR-125b-2 expression levels in patient's multiple myeloma cells from published dataset GSE39925. (C) qRT-PCR analysis of miR-125b-5p expression using total RNA from 24 primary patient MM cells, 10 MM cell lines and 3 samples of bone marrow-derived plasma cells from healthy donors (hd PCs). (D) MM were TC classified according to the presence of recurrent IGH chromosomal translocations and Cyclin D expression as previously described¹⁹, and miR-125b-5p expression in TC2 and TC3 subgroups is plotted. Raw Ct values were normalized to RNU44 housekeeping snoRNA and expressed as $2^{-\Delta Ct}$ values. Values represent mean \pm SE of three different experiments.

Figure 2. Anti-proliferative effects of miR-125b in MM cells. (A) qRT-PCR analysis of miR-125b-5p expression in SK-MM-1 cells transduced with either Lenti-miR-125b-1 or Lenti-miR-125b-2; the results are shown as average miR-125b-5p expression levels after normalization with RNU44 and $\Delta\Delta Ct$ calculations. (B) CCK-8 proliferation assay of NCI-H929, SK-MM-1 and RPMI-8226 cells transduced with a lentivirus carrying either the miR-125b-1 (Lenti-miR-125b-1) or the miR-125b-2 (Lenti-miR-125b-2) genes; the effects on cell proliferation were assessed at 2, 3 and 4 days after selection by puromycin. qRT-PCR analysis of miR-125b-5p expression in SK-MM-1 cells transfected with either (C) miR-125b-5p inhibitors or (E) miR-125b-5p mimics; the results are shown as average miR-125b-5p expression levels after normalization with RNU44 and $\Delta\Delta Ct$ calculations. (D) CCK-8 proliferation assay was performed 2-4 days after transfection of 8 MM cell lines (MM.1S, MM.1R, U266/LR7, RPMI-8226, RPMI-8226/DOX40, SK-MM-1, KMS-12-BM and INA-6) with miR-125b-5p inhibitors or scrambled controls (miR-NC inhibitors). (F) CCK-8 proliferation assay was performed 2-4 days after transfection of 10 MM cell lines (NCI-H929, U266, MM.1S, MM.1R, U266/LR7, RPMI-8226, RPMI-8226/DOX40, SK-MM-1, KMS-12-BM and INA-6) with miR-125b-5p mimics or scrambled controls (miR-NC mimics). (G) CCK-8 assay of CD138+ cells from 3 different MM patients transfected with miR-125b-5p or miR-NC. The assay was performed 48 hours after cell transfection. (H) 7-AAD flowcytometry assay was performed 48 hours after transfection of PBMCs from 7 healthy

donors (HDs) with miR-125b-5p or miR-NC. Data represent the average \pm SD of 3 independent experiments. P values were obtained using two-tailed *t* test.

Figure 3. IRF4 downregulation mediates miR-125b-5p anti-MM activity. (A) qRT-PCR analysis of IRF4 expression in SK-MM-1, NCI-H929 and RPMI-8226 cells 48 hours after transfection with miR-125b-5p or miR-NC. The results shown are average mRNA expression levels after normalization with GAPDH and $\Delta\Delta$ Ct calculations. (B) Western blot analysis of IRF4 in SK-MM-1, NCI-H929 and RPMI-8226 cells transfected with miR-125b-5p or miR-NC. Analysis was performed 24 and 48 hours after cell transfection. γ -Tubulin was used as protein loading control. (C) Western blot analysis of IRF4 in lysates from SK-MM-1 cells co-transfected with either IRF4 ORF expression vector or an empty vector and miR-125b-5p or miR-NC (48-hour time point). (D) CCK-8 assay of SK-MM-1 cells co-transfected with either IRF4 ORF expression vector or an empty vector and miR-125b-5p or miR-NC (48-hour time point). Data represent the average \pm SD of 3 independent experiments.

Figure 4. Impairment of IRF4 signaling by miR-125b-5p. (A) Western blot analysis of BLIMP-1 in SK-MM-1 cells transfected with miR-125b-5p or miR-NC. Analysis was performed 24 and 48 hours after cell transfection. γ -Tubulin was used as protein loading control. (B) Western blot analysis of BLIMP-1 in lysates from SK-MM-1 cells co-transfected with either BLIMP-1 ORF expression vector or IRF4 ORF expression vector or an empty vector and miR-125b-5p or miR-NC (48-hour time point). (C) CCK-8 assay of SK-MM-1 cells co-transfected with either BLIMP-1 ORF expression vector or an empty vector and miR-125b-5p or miR-NC (48-hour time point). (D) Western blot analysis of c-Myc, Casp-10 and cFLIP in SK-MM-1 cells transfected with miR-125b-5p or miR-NC. Analysis was performed 24 and 48 hours after cell transfection. GAPDH or γ -Tubulin were used as protein loading controls. (E) Western blot analysis of c-Myc, Casp-10 and cFLIP in lysates from SK-MM-1 cells co-transfected with either IRF4 ORF expression vector or an empty vector and miR-125b-5p or miR-NC (48-hour time point). GAPDH was used as protein loading control. All the experiments were performed in triplicate. Representative pictures are shown. (F) Esplanative cartoon of miR-125b-5p-mediated impairment of IRF4 signaling.

Figure 5. miR-125b-5p increases both apoptosis and autophagic efflux in MM cells.

(A) Annexin V / 7-AAD staining of SK-MM-1 cells transfected with miR-125b-5p or miR-NC. Flow cytometry analysis was performed 48-72 hours after transfection. (B) Western blot analysis of caspase-3 and caspase-8 activities in SK-MM-1 cells transfected with miR-125b-5p mimics or miR-NC. Analysis was performed 24-48 hours after cell transfection. γ -Tubulin or GAPDH were used as protein loading controls. (C) Annexin V/7-AAD staining of SK-MM-1 cells transfected with miR-125b-5p or miR-NC. 6 hours after electroporation either DMSO or zVAD-fmk were added to culture medium, at final concentration of 25 μ M. Flow cytometry analysis was performed 48 hours after transfection. (D) Cyto-ID uptake flow cytometry assay was performed in seven MM cell lines (NCI-H929, SK-MM-1, MM.1S, U266, RPMI-8226, XG-1 and INA-6) 48 hours after transfection with miR-125b-5p or miR-NC. (E) Western blot analysis of LC3B, Beclin-1 and p-62 was performed in XG-1 and SK-MM-1 cells transfected with miR-125b-5p or miR-NC. Analysis of LC3B and Beclin-1 was performed 24 hours after cell transfection, while analysis of p-62 was performed 48 hours after cell transfection. GAPDH was used as protein loading control. (F) Annexin V / 7-AAD staining of SK-MM-1 cells transfected with miR-125b-5p or miR-NC and then exposed to increasing concentrations (0-5-10-20 μ M) of the autophagy inhibitor cloroquine (added to culture medium 4 hours after electroporation). Flow cytometry analysis was performed 72 hours after transfection. All the experiments were performed in triplicate. Representative pictures are shown.

Figure 6. miR-125b-5p antagonizes pro-survival effect of BM milieu. (A) Quantitative RT-PCR of miR-125b-5p expression in NCI-H929, KMS-12-BM, INA-6, SK-MM-1 and U266 cells cultured in the presence or absence of either IL-6 (2.5 ng/mL) or IGF-1 (100 μ g/mL) or HGF (150 μ g/mL) (48 hours time-point). Raw Ct values were normalized to RNU44 housekeeping snoRNA and expressed as $\Delta\Delta$ Ct values calculated using the comparative cross threshold method. miR-125b-5p expression levels in cells cultured in the absence of growth factors were set as an internal reference. (B) Quantitative RT-PCR of miR-125b-5p expression in SK-MM-1 and U266 cells exposed to either DMSO or JQ1 (1 μ M) or 10058-F4 (100 μ M) (48 hours time point). Raw Ct values were normalized to RNU44 housekeeping snoRNA and expressed as $\Delta\Delta$ Ct values calculated using the comparative cross threshold method. miR-125b-5p expression levels in cells exposed to DMSO were set as an internal reference. (C) Quantitative RT-PCR of miR-125b-5p expression in SK-MM-1 cells cultured in the presence or absence of either IL-6 (2.5 ng/mL)

or IGF-1 (100 µg/mL) or HGF (150 µg/mL) and exposed to either DMSO or JQ1 (1µM) or 10058-F4 (100 µM) (48 hours time point). Raw Ct values were normalized to RNU44 housekeeping snoRNA and expressed as percentage of $\Delta\Delta$ Ct values calculated using the comparative cross threshold method. miR-125b-5p expression level in cells cultured in absence of growth factors and exposed to DMSO was set as an internal reference. **(D)** CCK-8 assay was performed 2 days after transfection of INA-6 and NCI-H929 cells with miR-125b-5p or miR-NC. IL-6 (2,5 ng/mL) or IGF-1 (100 ng/mL) or HGF (150 ng/mL) were added to complete culture medium. **(E)** 7-AAD flow cytometry assay of INA-6 and NCI-H929 cells cultured in the presence or absence of HS-5 / GFP+ stromal cell line. The assay was performed 48 hours after transfection of MM cells with miR-125b-5p mimics or miR-NC. To discriminate between MM cells and HS-5 stromal cells, GFP negative cells were gated. **(F)** Flow cytometry analysis of IL6-R/CD126 expression on cell surface of INA-6 cells after transfection with miR-125b-5p or miR-NC (48h time point). **(G)** Western blot analysis of total STAT3 (tSTAT3) and phosphorylated STAT3 (pSTAT3) in lysates from INA-6 cells transfected with miR-125b-5p or miR-NC (48h time point). GAPDH was used as protein loading control.

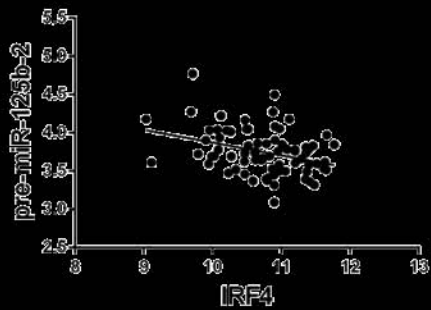
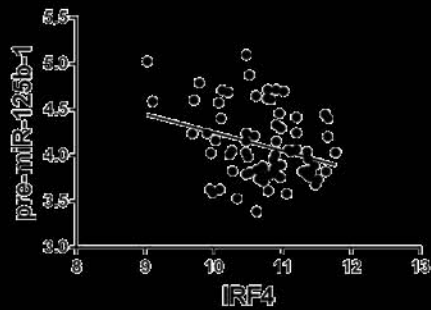
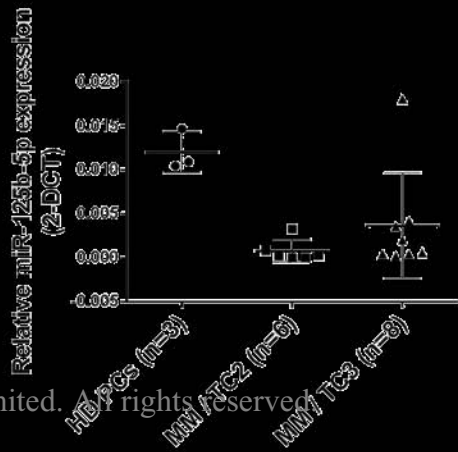
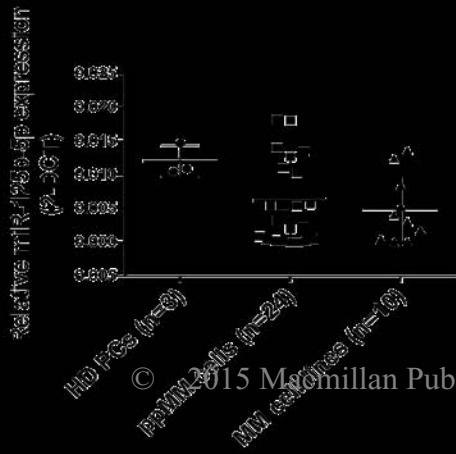
Figure 7. miR-125b-5p mimics antagonize MM tumor growth in vivo. In vivo growth of luciferase gene-marked NCI-H929 xenografts intra-tumorally treated with miR-125b-5p mimics or scr controls. Palpable subcutaneous tumor xenografts were treated with 20 mg of NLE-formulated oligos. Intra-tumor injections were administered every other day, for a total of 6 injections (indicated by arrows). **(A)** BLI-based measurement of tumor volumes (3 mice for each group) were made at 25 days from treatment. **(B)** Tumors were also measured with an electronic caliper every other day (5 mice for each group). Averaged tumor volume of each group \pm SD are shown. P values were obtained using two-tailed t test. **(C)** Survival curves (Kaplan–Meier) of intra-tumorally treated mice show prolongation of survival in miR-125b-5p-treated NCI-H929 xenografts compared with controls (log-rank test, $P < 0.05$). Survival was evaluated from the first day of treatment until death or sacrifice. Percentage of mice alive is shown. **(D)** In vivo tumor growth of NCI-H929 xenografts intra-peritoneally treated with NLE-formulated miR-125b-5p or miR-NC. Intra-peritoneal injections were administered twice/weekly, for a total of 4 injections (indicated by arrows). Tumors were measured with an electronic caliper every other day (5 mice for each group). Averaged tumor volume of each group \pm SD are shown. P values were obtained using two-tailed t test. **(E)** Survival curves (Kaplan–Meier) of intra-peritoneally

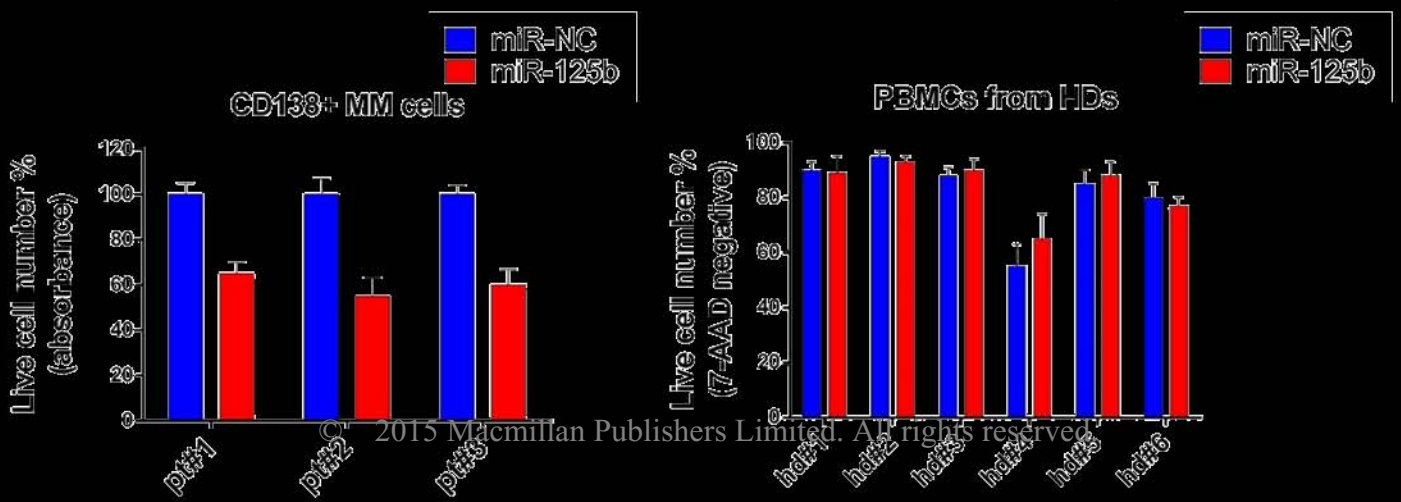
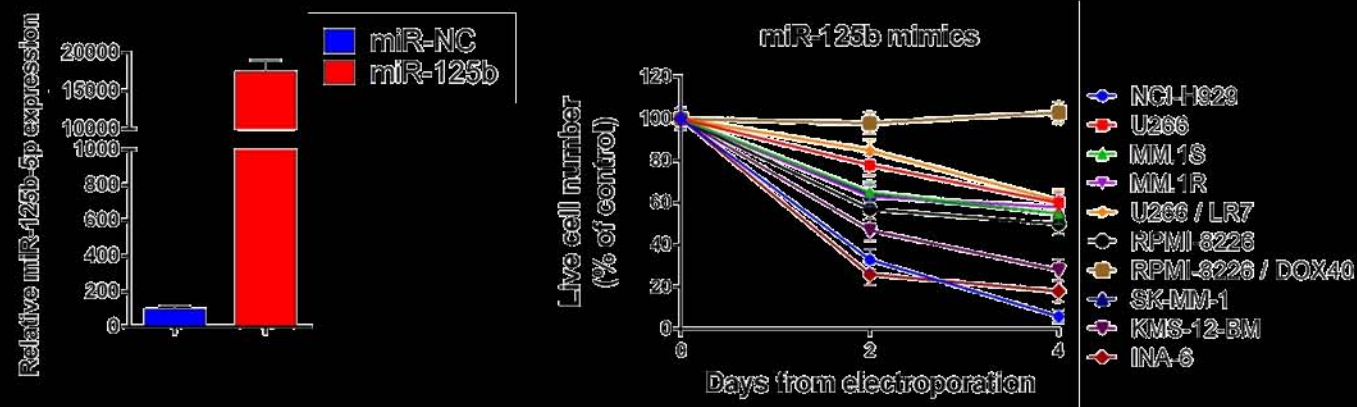
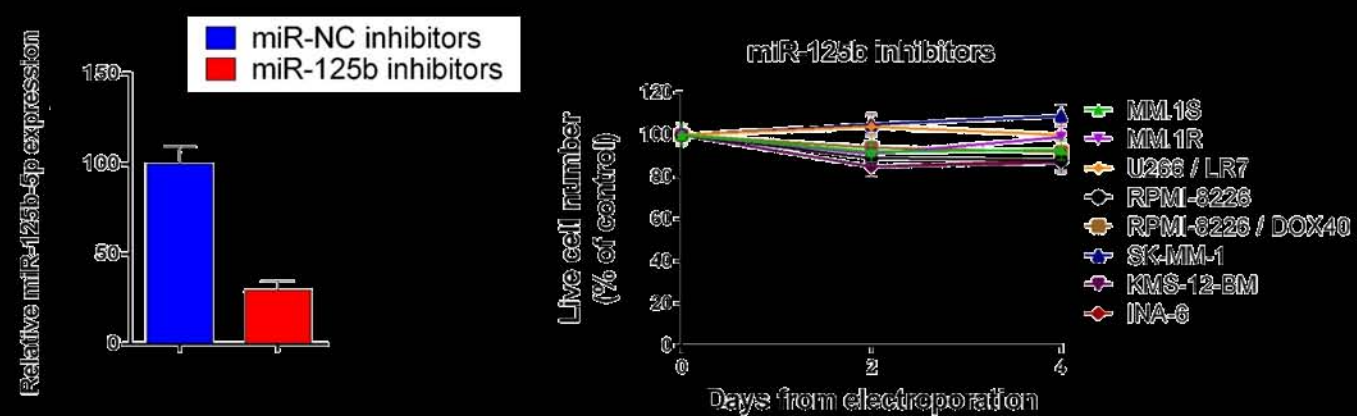
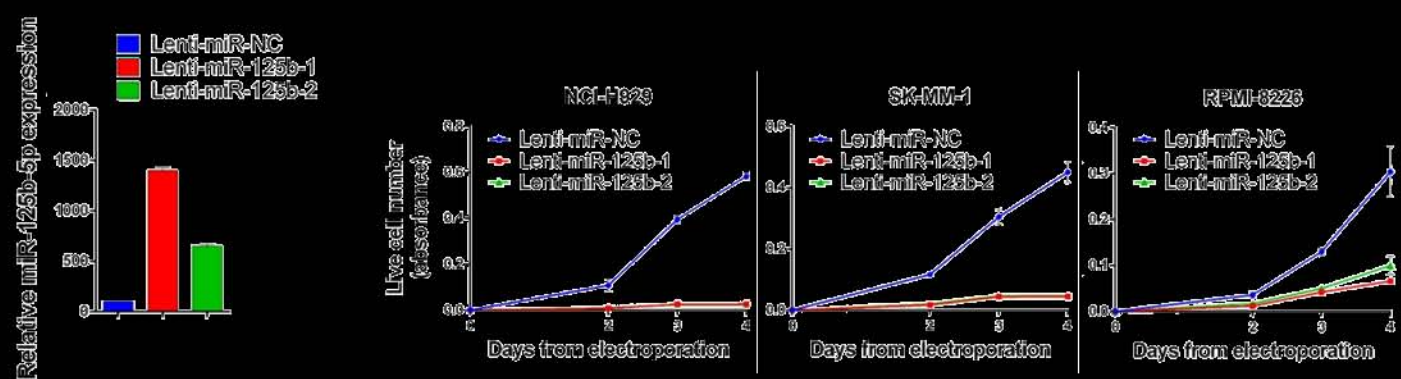
treated mice show prolongation of survival in miR-125b-5p–treated NCI-H929 xenografts compared with controls (log-rank test, $p < 0.05$). Survival was evaluated from the first day of treatment until death or sacrifice. Percentage of mice alive is shown. **(F)** qRT-PCR of miR-125b-5p expression in lysates from retrieved NCI-H929 xenografts intra-tumorally treated with miR-125b-5p or miR-NC. The results shown are average miRNA expression levels after normalization with RNU44 and $\Delta\Delta C_t$ calculations. Data represent the average \pm SD of 3 independent experiments. **(G)** Western blot analysis of BLIMP-1 and IRF4 in lysates from a representative retrieved NCI-H929 xenograft intra-tumorally treated with miR-125b-5p or miR-NC. GAPDH was used as protein loading control. **(H)** Western blot analysis of CASP10, cFLIP and c-Myc in lysates from a representative retrieved NCI-H929 xenografts intra-tumorally treated with miR-125b-5p or miR-NC. GAPDH was used as protein loading control.

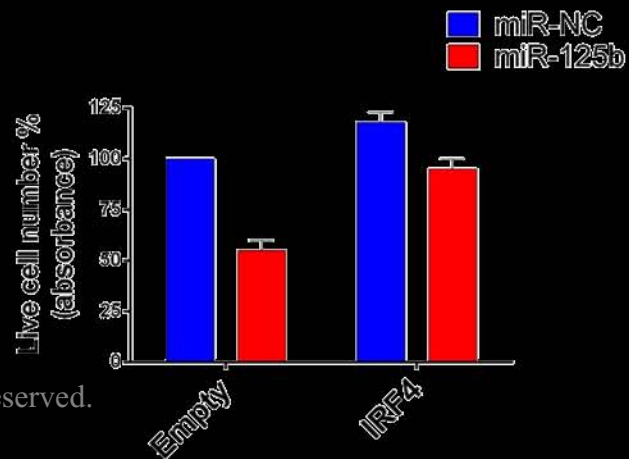
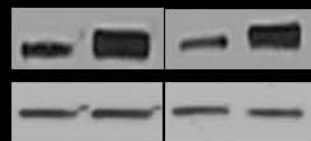
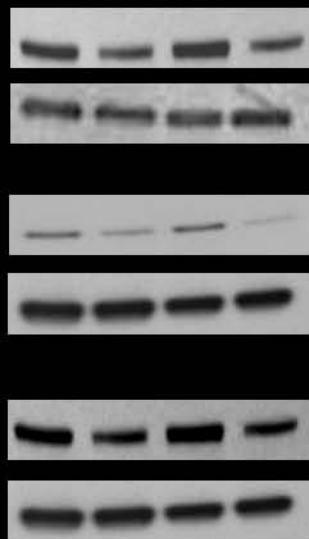
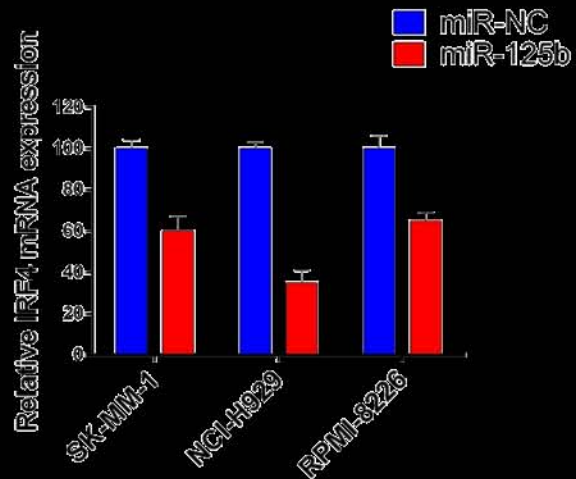
Accepted manuscript

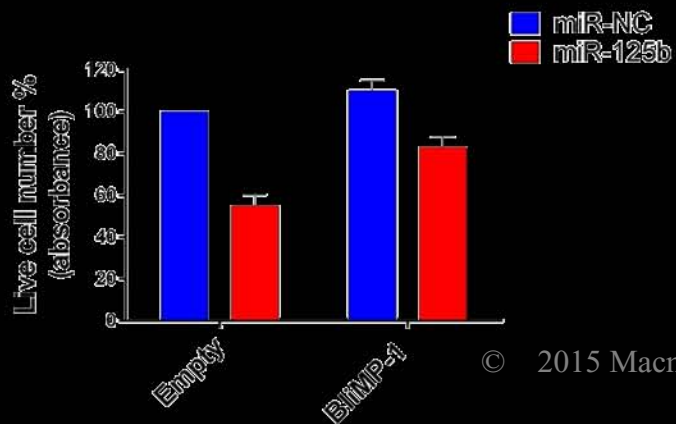
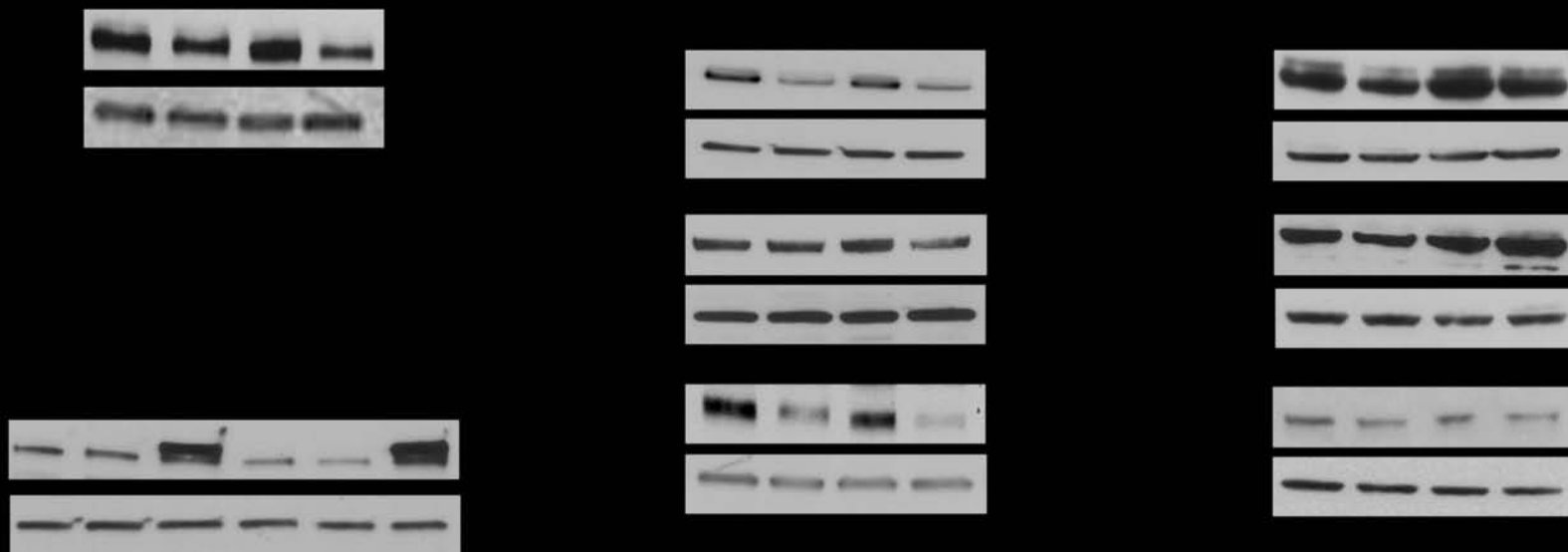
Table1. *In silico* search for IRF4-targeting miRNAs

Gene	microRNA	Source	Score (std)
IRF4	hsa-mir-125a-5p	picTar_ver2_hg18_Mar2006_mammals	4.52261
IRF4	hsa-mir-125b-5p	picTar_ver2_hg18_Mar2006_mammals	5.02513
IRF4	hsa-mir-128	picTar_ver2_hg18_Mar2006_mammals	3.51759
IRF4	hsa-mir-27a-3p	picTar_ver2_hg18_Mar2006_mammals	5.02513
IRF4	hsa-mir-27b-3p	picTar_ver2_hg18_Mar2006_mammals	6.03015
IRF4	hsa-mir-30a-5p	picTar_ver2_hg18_Mar2006_mammals	2.01005
IRF4	hsa-mir-30b-5p	picTar_ver2_hg18_Mar2006_mammals	1.00503
IRF4	hsa-mir-30c-2	picTar_ver2_hg18_Mar2006_mammals	1.00503
IRF4	hsa-mir-30d-5p	picTar_ver2_hg18_Mar2006_mammals	2.51256
IRF4	hsa-mir-30e-5p	picTar_ver2_hg18_Mar2006_mammals	4.52261
IRF4	hsa-mir-4319	picTar_ver2_hg18_Mar2006_mammals	14.5729
IRF4	hsa-mir-513a-5p	picTar_ver2_hg18_Mar2006_mammals	14.0704

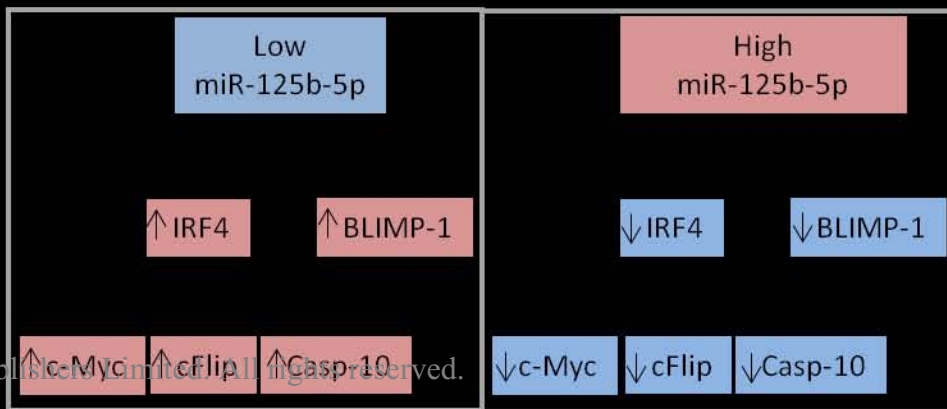


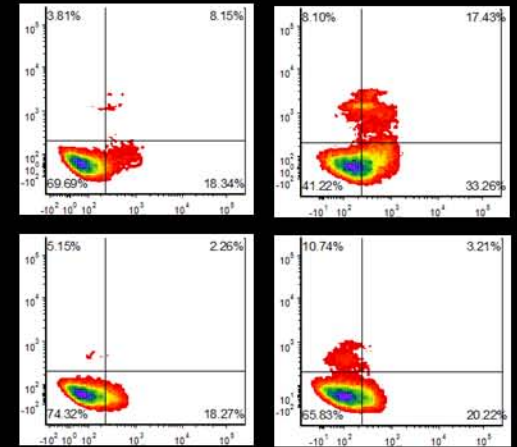
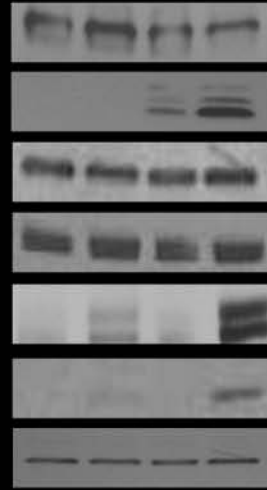
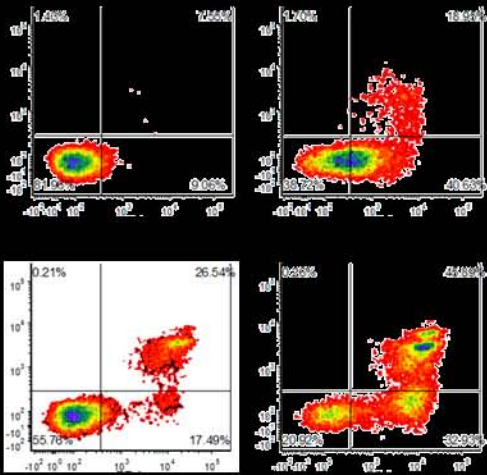






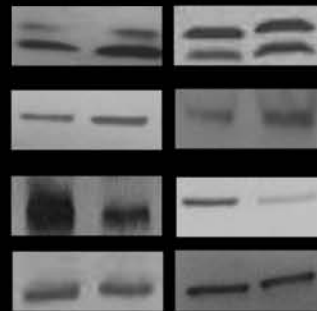
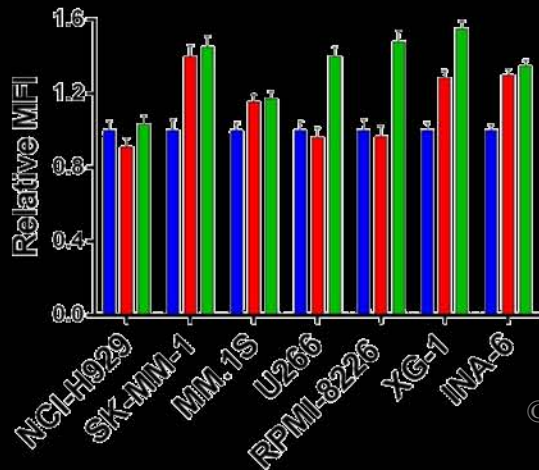
© 2015 Macmillan Publishers Limited. All rights reserved.





Cyto-ID uptake

miR-NC miR-125b starvation



Annexin V staining

